

Review

Metasurface-Enabled Microphotonic Biosensors via BIC Modes

Francesco Dell'Olio 

Micro Nano Sensor Group, Polytechnic University of Bari, 70126 Bari, Italy; francesco.dellolio@poliba.it

Abstract: Photonic biosensors based on bound states in the continuum (BIC) resonant modes exhibit a transformative potential for high-sensitivity, label-free detection across various diagnostic applications. BIC-enabled metasurfaces, utilizing dielectric, plasmonic, and hybrid structures, achieve ultra-high Q-factors and amplify target molecule interactions on functionalized sensor surfaces. These unique properties result in increased refractive index sensitivity and low detection limits, essential for monitoring biomolecules in clinical diagnostics, environmental analysis, and food safety. Recent advancements in BIC-enabled metasurfaces have demonstrated ultra-low detection limits in the zeptomolar range, making these devices highly promising for real-world applications. This review paper critically discusses the design principles of BIC-based biosensors, emphasizing key factors such as material selection, structural asymmetry, and functionalization strategies that enhance both sensitivity and specificity. Additionally, recent advancements in fabrication techniques that enable precise BIC control with scalable approaches for practical biosensing applications are examined. Case studies demonstrate the effectiveness of BIC metasurfaces for real-time, low-concentration detection, highlighting their versatility and adaptability. Finally, the review discusses future challenges and opportunities, such as integration with microfluidics for point-of-care testing and multiplexed sensing, underscoring the potential of BIC-based platforms to revolutionize the field of biosensing.

Keywords: nanophotonics; metasurface; biosensing; label-free detection; point-of-care diagnostics



Received: 30 November 2024

Revised: 19 December 2024

Accepted: 6 January 2025

Published: 8 January 2025

Citation: Dell'Olio, F. Metasurface-Enabled Microphotonic Biosensors via BIC Modes. *Photonics* **2025**, *12*, 48. <https://doi.org/10.3390/photonics12010048>

Copyright: © 2025 by the author. Licensee MDPI, Basel, Switzerland. This article is an open access article distributed under the terms and conditions of the Creative Commons Attribution (CC BY) license (<https://creativecommons.org/licenses/by/4.0/>).

1. Introduction

Biosensors are analytical devices designed to detect biological molecules, which integrate a biorecognition element with a signal transducer. They hold immense potential across healthcare, biodefense, environmental monitoring, and food safety, driven by the ongoing demand for rapid, accurate, and cost-effective diagnostics [1]. Current research focuses on achieving three key goals: (i) integration into point-of-care testing (PoCT) systems comprising low-cost disposable biochips and simple reader devices; (ii) ultra-low limits of detection (LoDs) that extend down to the zeptomolar (zM) range; and (iii) ultra-wide detection ranges spanning, for example, from zM to picomolar (pM) concentrations. These objectives are pursued alongside standard requirements such as selectivity, specificity, stability, and reproducibility. Among biosensors, optical chip-scale platforms exhibit unique advantages in addressing these challenges. Their label-free detection capabilities, high sensitivity, and compatibility with CMOS fabrication processes make them ideal for miniaturized, portable PoCT applications. Silicon photonic biosensors [2,3], such as those developed by SiPhox and Genalyte, exemplify this trend. SiPhox leverages silicon photonic ring resonators to measure biomarkers, such as high-sensitivity C-reactive protein, with compact reader instruments, while Genalyte's Maverick system integrates multiplexed

detection with cloud connectivity for advanced diagnostics. These platforms demonstrate the feasibility of high-performance biosensors within disposable and user-friendly systems. The development of chip-scale optical biosensors offers a promising pathway toward fulfilling the ambitious goals of modern biosensing. By enabling precise and scalable integration of biosensing functions, these devices pave the way for transformative advances in diagnostics.

Metasurfaces—thin layers composed of subwavelength nanostructures arranged according to periodic or pseudo-periodic grids—have demonstrated remarkable potential in controlling the behavior of electromagnetic waves, enabling precise manipulation of light properties such as phase, amplitude, and polarization [4–12]. By tailoring the geometry, size, and arrangement of these nanostructures, metasurfaces can achieve effects that traditionally require much thicker optical components, thus paving the way for highly compact, lightweight, and versatile optical devices. Among the various resonant phenomena that can be engineered within metasurfaces, BICs have emerged as particularly promising because of their unique ability to provide high-Q resonances. This feature makes BICs highly suitable for applications requiring extreme sensitivity and strong light–matter interaction, such as biosensing [13–16].

BICs are distinctive, resonant states that remain perfectly confined within a radiation continuum, thus achieving theoretically infinite quality factors [17–19]. Unlike typical resonant modes, which tend to couple with external radiation and lose energy, BICs avoid such coupling by virtue of symmetry constraints or destructive interference mechanisms. This enables them to retain energy without radiation leakage, resulting in confined resonances that are exceptionally sharp and robust against radiative decay. As illustrated in Figure 1, BICs reside in the radiation continuum without coupling to radiative modes, producing enhanced field localization that is beneficial for applications requiring intense light–matter interactions. This intrinsic property has spurred substantial interest in BIC-based metasurfaces across multiple fields, from lasing and nonlinear optics to sensing and imaging.

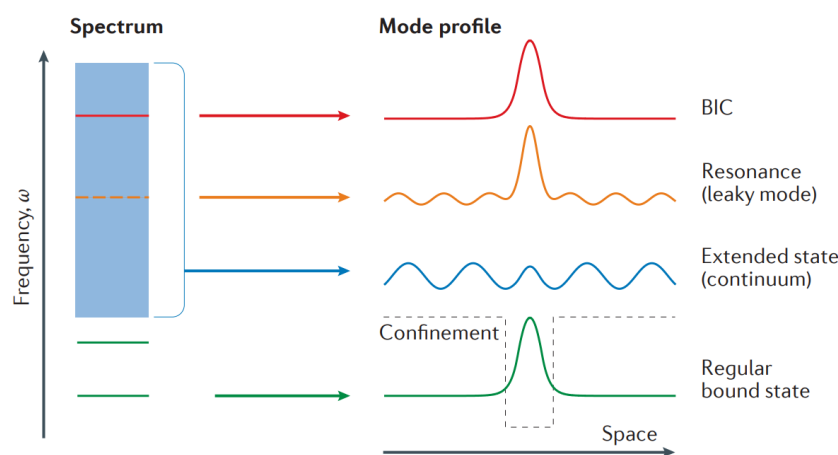


Figure 1. Illustrative concept of BICs. Within an open system, the frequency spectrum includes a continuum of extended states (blue) and discrete bound states (green) that do not radiate. Structures with specific symmetry and interference properties enable BICs (red), which reside within the continuum but remain localized without energy loss. Reprinted with permission from [17].

The high-Q resonances achievable on BIC-based metasurfaces are particularly advantageous for biosensing applications, where a sensor’s performance is often determined by its sensitivity to changes in the refractive index near the sensing surface. High-Q BIC resonances amplify the interaction between incident light and analytes within the functionalized sensing region, significantly enhancing the sensor’s response to minute

changes in refractive index [20,21]. This sensitivity is critical in detecting low concentrations of biomolecules—such as proteins, DNA, and other biomarkers—that might be indicative of disease states. Additionally, the high-Q nature of BICs reduces the linewidth of the resonance, leading to improved signal-to-noise ratios that are essential for high-precision biosensing.

Similarly to other chip-scale technologies, a further advantage of BIC-based biosensors is their capability for label-free detection. Traditional biosensing methods often require fluorescent or colorimetric labels to visualize molecular interactions, which can add complexity and limit the application scope. BIC-based sensors, however, achieve strong field localization within the active sensing layer, enabling the direct detection of biomolecules without the need for additional labels. This label-free approach not only simplifies the sensing process but also enables real-time monitoring of biological interactions, an important feature in diagnostic and environmental sensing applications.

BIC-based metasurfaces exploit a very simple excitation scheme, which is normal-to-surface. As shown in Figure 2, the metasurface is typically excited by a beam that is normal to the surface, and reflection and transmission spectra are observed. The metasurface supports a BIC-wave that is delocalized in a wide area, thus enhancing light–matter interaction.

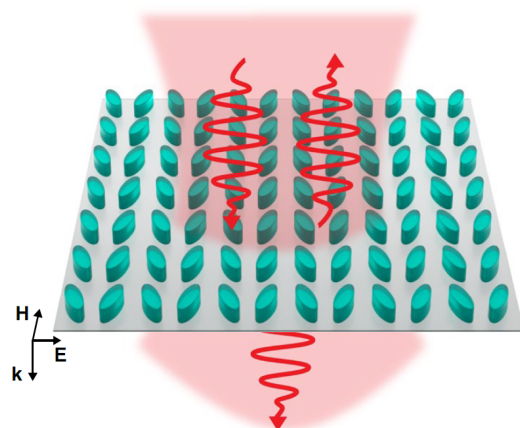


Figure 2. Light scattered by the metasurface. The metasurface is top-illuminated. Reflection and transmission can be observed. The metasurface is a periodic 2D array of dielectric metaunits, each consisting of a pair of tilted silicon nanobars. Each metaunit has a mirror symmetry across the major vertical axis and consists of elliptical dielectric nanoresonators with major and minor axes of approximately 280 nm and 100 nm, respectively. These dimensions are fine-tuned to achieve the desired resonance wavelength. The all-dielectric metasurface was fabricated by nanopatterning a thin layer (100 nm) of amorphous silicon, which was deposited on a fused-silica substrate. Reprinted with permission from [22].

The versatility of BIC-based metasurfaces is enhanced by the range of material choices available, including dielectric, plasmonic, and hybrid metal–dielectric materials. Dielectric metasurfaces, for instance, offer low-loss, high-Q resonances due to minimal intrinsic absorption, making them ideal for applications where high sensitivity and stability are paramount. Plasmonic metasurfaces, which utilize metals such as gold or silver, provide strong field enhancement near the metal surface, making them well-suited for applications requiring intense local field effects. However, their intrinsic losses can limit the achievable Q-factors. Hybrid metal–dielectric BIC metasurfaces represent a promising compromise, combining the strong field localization of plasmonic structures with the low-loss advantages of dielectric materials. This flexibility allows BIC-based sensors to be tailored to specific application requirements, optimizing parameters such as sensitivity, robustness, and compatibility with lab-on-chip platforms [23–26].

This review explores the principles and applications of BIC-based metasurfaces for biosensing. The focus is on metasurfaces that operate in the visible and infrared spectral regions, where BIC resonances are particularly relevant for optical biosensing applications. Several metasurfaces for biosensing that support BIC have been demonstrated in the THz regime, achieving an LoD as low as a few tens of aM [27–29]. Section 2 delves into the mechanisms behind BIC resonances in metasurfaces, providing an overview of symmetry-protected, Friedrich–Wintgen, and Fabry–Perot BICs. Section 3 examines the key design parameters that are essential for maximizing sensitivity and specificity in BIC-based biosensors, including refractive index sensitivity, material choice, and functionalization techniques. Section 4 discusses the fabrication techniques and challenges associated with producing high-Q BIC metasurfaces. Section 5 highlights applications of BIC-based biosensors in clinical diagnostics and environmental monitoring, emphasizing performance benchmarks. Finally, Section 6 outlines potential future developments and challenges for BIC-based biosensing technologies.

2. Principles of BIC Resonance in Metasurfaces

The BIC phenomenon occurs due to specific conditions of symmetry and interference that prevent coupling with radiative modes, allowing for high field confinement within the metasurface structure [30–33]. BICs, originally introduced in quantum mechanics, have become a fundamental concept in nanophotonics and are utilized in various applications, including enhanced biosensing, which is the topic of this review paper.

BICs can be categorized into three primary types based on their mechanisms of confinement: symmetry-protected BICs [34–36], Friedrich–Wintgen (or accidental) BICs [37–39], and Fabry–Perot BICs [40–42]. Symmetry-protected BICs arise in systems where the confined mode's symmetry prevents it from coupling with the radiative continuum. In metasurfaces, this form of BIC typically occurs in symmetric structures where the symmetry of the mode is incompatible with the surrounding radiation modes. This symmetry mismatch results in a non-radiating state that remains perfectly confined. When the symmetry of these structures is intentionally broken, the symmetry-protected BIC transitions to a quasi-BIC (qBIC), introducing a controlled level of radiative leakage. This slight asymmetry enables the creation of ultra-high-Q resonances that retain much of the confinement characteristics of a pure BIC, making them suitable for experimental applications where complete isolation is not feasible. Friedrich–Wintgen BICs, named after the physicists who first identified this mechanism, rely on destructive interference between two or more resonant modes, resulting in a non-radiating state within the continuum. This type of BIC does not depend on the system's symmetry but instead occurs due to phase-matching conditions that allow multiple resonances to cancel each other's radiative components. Fabry–Perot BICs, on the other hand, emerge in periodic or multilayer structures where phase-matching conditions lead to constructive interference within the structure, effectively confining light due to balanced internal and external phase conditions. These BICs are particularly relevant in multilayer and waveguide structures, where they exploit internal reflection mechanisms to achieve confinement.

The ability to confine light within a metasurface structure using BICs has profound implications for enhancing light–matter interactions. This high-Q resonance produces a stronger electromagnetic field within the region of confinement, which is particularly advantageous for applications like biosensing that rely on detecting minute changes in refractive index. By focusing light within a small volume, BICs amplify the interaction between light and biomolecules, increasing sensitivity to low concentrations of analytes. The enhancement of the electromagnetic field within the metasurface also enables label-free detection, as it eliminates the need for external tags or markers to visualize biomolecular interactions.

BICs can be realized in dielectric, plasmonic, and metal–dielectric hybrid metasurfaces, each offering distinct advantages based on their material properties and resonant behaviors.

Dielectric metasurfaces, typically composed of materials like silicon or titanium dioxide, are particularly well-suited for supporting high-Q BICs due to their low intrinsic optical losses. At the state-of-the-art, the highest Q-factor in such BIC-supporting metasurfaces is close to 500,000 [43]. Dielectric materials facilitate the generation of Mie resonances, which allow for strong confinement of electromagnetic fields within the nanostructure while minimizing dissipative losses. This characteristic makes dielectric metasurfaces ideal for applications demanding high sensitivity and stability, such as biosensors designed to detect minute changes in refractive index or low concentrations of analytes. The ability to achieve ultra-narrow resonance linewidths further enhances their precision and signal-to-noise ratio, making them a cornerstone in the development of advanced BIC-based sensing platforms.

Plasmonic metasurfaces, in contrast, rely on metallic materials such as gold, silver, or aluminum to harness surface plasmon resonance (SPR). These metasurfaces exhibit exceptionally strong near-field enhancement due to the collective oscillation of free electrons at the metal–dielectric interface when illuminated by light at specific wavelengths. While plasmonic metasurfaces inherently suffer from higher intrinsic losses compared with their dielectric counterparts, the intense field localization near the metallic nanostructures can significantly amplify light–matter interactions. This property is especially advantageous for applications that prioritize strong surface sensitivity, such as label-free biosensing and surface-enhanced Raman spectroscopy. For instance, plasmonic metasurfaces have been shown to detect low concentrations of biomolecules by leveraging their capacity to amplify the electromagnetic field within the sensing region, albeit at the expense of broader resonance linewidths and reduced Q-factors.

Metal–dielectric hybrid metasurfaces bridge the gap between these two paradigms by combining the high-field localization of plasmonic materials with the low-loss characteristics of dielectric components. These hybrid designs enable the realization of quasi-BICs that offer a balance between field confinement and radiative leakage. By integrating plasmonic nanostructures with dielectric layers, hybrid metasurfaces can achieve enhanced near-field interactions while maintaining relatively narrow resonance linewidths compared to purely plasmonic systems. This synergy is particularly valuable for biosensing applications where both high sensitivity and robustness are required. For example, hybrid metasurfaces can be tailored to operate at specific wavelengths, optimizing the trade-off between sensitivity and Q-factor to meet the needs of diverse sensing scenarios.

The choice between dielectric, plasmonic, or hybrid metasurfaces depends on the specific requirements of the application. Dielectric metasurfaces excel in scenarios where minimizing energy loss and achieving high-Q resonances are critical, making them suitable for high-precision sensing. Plasmonic metasurfaces are preferred for applications demanding extreme near-field enhancement and strong surface interactions, despite their higher losses. Hybrid metasurfaces offer a versatile alternative, leveraging the strengths of both approaches to deliver tailored solutions for demanding biosensing environments. This versatility highlights the importance of material and structural optimization in designing metasurfaces that maximize the advantages of BICs across a broad range of applications.

As already mentioned, structural asymmetry plays a critical role in tuning the Q-factor and resonance properties of BICs, particularly in the generation of quasi-BICs. Introducing a slight asymmetry in a BIC-supporting structure—such as altering the shape, refractive index, or periodicity of the nanostructures—results in a quasi-BIC with finite but high Q-factors. This controlled asymmetry allows for selective coupling with radiative modes, enabling external access to the confined mode without fully compromising its

resonant characteristics. For biosensing applications, the ability to fine-tune the Q-factor by adjusting the degree of asymmetry is essential for optimizing sensitivity to refractive index changes. Quasi-BICs created through asymmetry adjustments offer a practical approach for enhancing the detection of biomolecular interactions within the functionalization layer of the sensor. By designing the asymmetry to achieve a specific resonance linewidth, quasi-BICs provide high field localization with a controlled level of radiation, balancing confinement with accessibility.

Figure 3 illustrates the impact of introducing asymmetry in metasurfaces designed to support BICs, taking as an example the metasurface discussed in [44]. The figure demonstrates how varying the asymmetry parameter d_x , from $d_x = 0$ nm (symmetric configuration) to $d_x = 120$ nm (asymmetric configuration), influences the transition from pure BICs to quasi-BICs (qBICs). In the symmetric case, the metasurface supports BICs that are perfectly confined without radiative losses, leading to theoretically infinite Q-factors. As asymmetry increases, controlled radiation leakage is introduced, transforming the BICs into qBICs with finite yet high Q-factors. This tunable balance between field confinement and radiative coupling in qBICs is particularly advantageous for biosensing applications, as it allows for high sensitivity while maintaining practical detection capabilities.

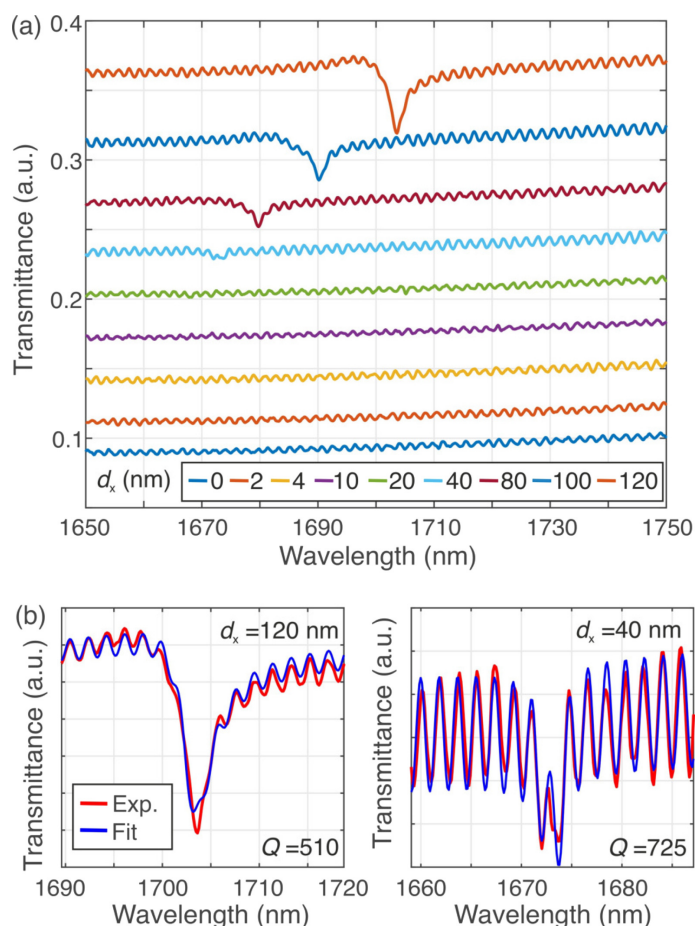


Figure 3. Illustration of the transition from BICs to qBICs in a metasurface as the asymmetry parameter d_x varies. For $d_x = 0$ nm (symmetric case), the metasurface supports perfectly confined BICs with infinite Q-factors. As d_x increases to 120 nm, qBICs emerge with controlled leakage and finite Q-factors, balancing field confinement and radiative coupling. This tunable behavior highlights the potential of such metasurfaces for applications requiring both sensitivity and accessibility, such as biosensing. (a) Experimentally measured transmittance spectra. (b) Spectra for $d_x = 40$ nm and $d_x = 120$ nm with the relevant fit. Reprinted with permission from [44].

3. Design Considerations for BIC-Based Biosensors

The design of BIC-based biosensors requires careful optimization of some parameters of the metasurface, such as refractive index sensitivity, field confinement where the target–receptor molecular interaction takes place, Q-factor of the BIC mode, and figure of merit (FOM), defined as the sensitivity-to-linewidth ratio. These parameters collectively determine the sensor’s performance in detecting small refractive index changes, which is essential for biosensing. In BIC-based sensors, the refractive index sensitivity typically ranges between 100 and 500 nm/RIU, with high-Q resonances yielding experimental values above 1000 [45]. The FOM, expressed in RIU^{-1} , reaches values exceeding 100 RIU^{-1} for optimized BIC structures. This high FOM, together with the field confinement close to the sensor surface exposed to the target molecules, is crucial for achieving precise detection, as it balances sensitivity with spectral resolution. The measured Q-factor, Q_{tot} , has a significant impact on the LoD, as described by the following equation:

$$\text{LoD} = \frac{\lambda_0}{S Q_{\text{tot}} \left(\frac{Q_{\text{tot}}}{Q_{\text{R}}} \right)} \sqrt{3\sigma}, \quad (1)$$

where λ_0 is the resonance wavelength, S is the sensitivity (nm/RIU), Q_{tot} is the measured total quality factor, and Q_{R} is the resonant Q-factor, i.e., the quality factor without losses. The term σ represents the noise variance. This equation highlights that the LoD decreases as Q_{tot} increases, underscoring the critical role of achieving high-Q resonances to resolve minute shifts in the resonance wavelength. For a more detailed discussion, refer to Ref. [46].

The selection of materials and geometric optimization play pivotal roles in maximizing the Q-factor and enhancing the refractive index sensitivity. Dielectric materials are preferred due to their low intrinsic losses and capability to support high-Q resonances with minimal energy dissipation. Conversely, hybrid metal–dielectric structures, which incorporate plasmonic materials like gold or silver, offer enhanced near-field interactions, albeit at the cost of slightly reduced Q-factors, typically in the order of some hundreds [47]. These hybrid designs are useful in applications where field enhancement near the sensor surface is prioritized, even if higher radiative losses are introduced.

Specificity in biosensing applications relies on functionalization strategies that ensure selective binding of target analytes. Functionalization methods often involve biochemical receptors such as antibodies, aptamers, or molecularly imprinted polymers (MIPs) tailored to interact specifically with the target molecule. The strong field confinement provided by BICs enhances the interaction between the target analyte and the functionalized surface, improving signal response and enabling low-concentration detection without the need for labeling agents.

Case studies of BIC-based biosensors demonstrate their effectiveness in real-time monitoring and low-concentration analyte detection. They will be discussed in Section 5.

Simulation Techniques for BIC-Based Metasurfaces

The design and optimization of metasurfaces supporting BICs heavily rely on advanced numerical simulation techniques. These methods allow for the detailed exploration of electromagnetic behavior, facilitating the tailoring of metasurface properties to achieve high sensitivity, Q-factors, and field confinement. Key simulation methods include rigorous coupled-wave analysis (RCWA), finite-difference time-domain (FDTD), finite element method (FEM), and eigenmode solvers.

RCWA [48–52] is a frequency-domain method particularly well-suited for analyzing periodic structures such as metasurfaces. By expanding the electromagnetic fields into Fourier series, RCWA provides a computationally efficient way to study the diffraction behavior and resonance characteristics of periodic structures. This method is highly effec-

tive for analyzing the optical response of BIC metasurfaces, particularly their reflectance, transmittance, and resonance sharpness. RCWA is frequently used in the initial stages of design to evaluate the influence of lattice parameters, feature dimensions, and material properties on the emergence of BICs and quasi-BICs (qBICs).

The FDTD method is widely employed for simulating the dynamic interaction of light with metasurfaces. Solving Maxwell's equations in the time domain, FDTD enables the detailed analysis of transient and steady-state field distributions. This method is particularly useful for visualizing field localization near BIC modes and optimizing the geometric parameters for maximum sensitivity and Q-factor. FDTD simulations are also critical for studying the effect of symmetry-breaking perturbations on the transition from BIC to qBIC modes.

The FEM is another widely used approach, particularly for metasurfaces with complex geometries or inhomogeneous material properties. FEM operates in the frequency domain, dividing the computational space into finite elements and solving Maxwell's equations locally. This method is ideal for detailed studies of near-field distributions, coupling effects, and the impact of material anisotropy on the BIC properties.

Eigenmode solvers are crucial for the direct identification and analysis of BIC modes in metasurfaces. By solving for the eigenfrequencies and eigenfields, these solvers help determine the conditions under which BICs occur, quantify Q-factors, and predict how structural parameters affect radiative losses and resonance tunability. This approach provides a robust framework for understanding the transition from pure BICs to qBICs under controlled symmetry-breaking.

The simulation process for BIC metasurfaces often involves a combination of these methods. RCWA provides rapid initial analyses of periodic structures, while FDTD and FEM offer more detailed insights into electromagnetic field behavior and resonance optimization. Eigenmode solvers complement these techniques by providing direct access to mode characteristics and guiding the design toward specific application requirements.

Environmental and mechanical considerations, such as temperature variations or substrate deformation, can also influence the performance of BIC-based sensors. Multiphysics simulation platforms that integrate optical, thermal, and mechanical modeling enable the prediction of sensor behavior under real-world conditions, ensuring robust designs for practical applications.

4. Fabrication Techniques, Functionalization, and Microfluidic Integration Challenges

The fabrication of BIC-based metasurfaces relies on precise nanofabrication techniques to achieve the high structural fidelity necessary for supporting high-Q resonances. In fact, the Q-factor is limited by the fabrication imperfections and the finite size of the metasurface, in addition to the light absorption by the non-transparent media where the electromagnetic field is confined and the angular spread collimated beam utilized for the metasurface excitation.

Commonly employed methods for metasurfaces fabrication include electron beam lithography (E-beam lithography), focused ion beam (FIB) milling, and nanoimprint lithography (NIL). Each technique offers unique advantages and faces distinct challenges when applied to the production of BIC metasurfaces for biosensing applications. This section explores these fabrication techniques, addressing the challenges in achieving reproducible, high-Q BICs, and the importance of material selection in maintaining BIC quality over large sensor areas.

E-beam lithography is widely used for the fabrication of BIC metasurfaces due to its high resolution and precise control over nanoscale features. This technique allows

for the direct writing of patterns on a substrate by using a focused electron beam to expose a resist layer, which is subsequently developed to reveal the desired nanostructures. E-beam lithography is particularly effective for creating the fine features and complex geometries required for BIC formation, such as symmetry-breaking elements that enable quasi-BICs (qBICs) with controlled radiative losses. However, E-beam lithography is limited by its low throughput and high cost, making it less suitable for large-scale production. Achieving reproducibility over large areas is challenging with E-beam lithography, as variations in exposure dose and development conditions can lead to inconsistencies in feature dimensions, which directly affect the Q-factor of BICs.

FIB milling is another technique employed in the fabrication of BIC metasurfaces. FIB uses a focused beam of ions, typically gallium, to sputter material from the surface, allowing for direct patterning of nanostructures without the need for a resist layer. FIB milling offers flexibility in pattern design and is well-suited for rapid prototyping and the fabrication of complex structures. However, like E-beam lithography, FIB is limited in scalability and throughput. Additionally, the high energy of ion milling can introduce damage to the material, potentially reducing the quality of the BIC resonance due to structural imperfections and material degradation.

Nanoimprint lithography (NIL) has emerged as a highly versatile and promising method for the large-scale fabrication of metasurfaces based on bound states in the continuum (BIC), particularly for applications requiring extensive biosensing areas [53–56]. This technique employs a pre-patterned mold to replicate nanoscale structures onto a substrate. By applying heat and pressure, the resist layer conforms to the mold's intricate patterns, enabling the creation of highly precise and complex geometries. NIL offers significant advantages, including high throughput and reduced costs compared to techniques like electron-beam lithography. Recent research has demonstrated that NIL can achieve nanoscale features with accuracies comparable to those produced by electron-beam lithography while offering greater scalability. However, NIL also faces technical challenges. The precision of the process is critically dependent on the quality of the mold and the uniform distribution of pressure during the imprinting phase. Minor imperfections in the mold or uneven pressure can lead to inconsistencies in feature dimensions and shapes, which may degrade the quality of BIC resonances by introducing scattering losses and lowering the Q-factor. Furthermore, the materials used in NIL must withstand the mechanical and thermal stresses of the process, which narrows the range of suitable materials for fabricating BIC metasurfaces.

The choice of fabrication technique has a profound impact on the performance of BIC-based biosensors. While E-beam lithography and FIB milling provide high precision, their scalability is limited, making NIL a more promising option for producing large-area BIC metasurfaces at scale. However, achieving consistent high-Q performance across large areas remains a challenge that requires continued research into material stability, process optimization, and mold fabrication for NIL.

Surface functionalization is a critical step in transforming a fabricated metasurface into a functional biosensor. One commonly employed protocol utilized for all-dielectric silicon or silicon nitride metasurfaces involves silanization followed by the application of a crosslinker to immobilize biorecognition elements. The surface is functionalized and incubated with aptamers or antibodies specific to the target analyte, ensuring covalent binding. This approach enables the precise detection of biomolecular interactions.

Integration with microfluidic systems is equally essential for real-time sensing applications. PDMS-based microfluidic chambers are typically plasma-bonded to the metasurface. The chamber features inlet and outlet ports for controlled fluid injection and allows the metasurface to interact with analytes in a liquid environment. This approach facilitates

precise monitoring of molecular binding events, crucial for biosensing applications. The chamber should be optimized to ensure compatibility with high-Q metasurface resonance conditions, especially minimizing signal perturbations caused by flow-induced stress.

To provide a clear summary of the key processes involved, Figure 4 illustrates the fabrication, functionalization, and microfluidic integration steps for BIC-based metasurfaces. This schematic offers an overview of the methodologies described in this section, highlighting the critical stages required to manufacture these biosensors for practical applications.

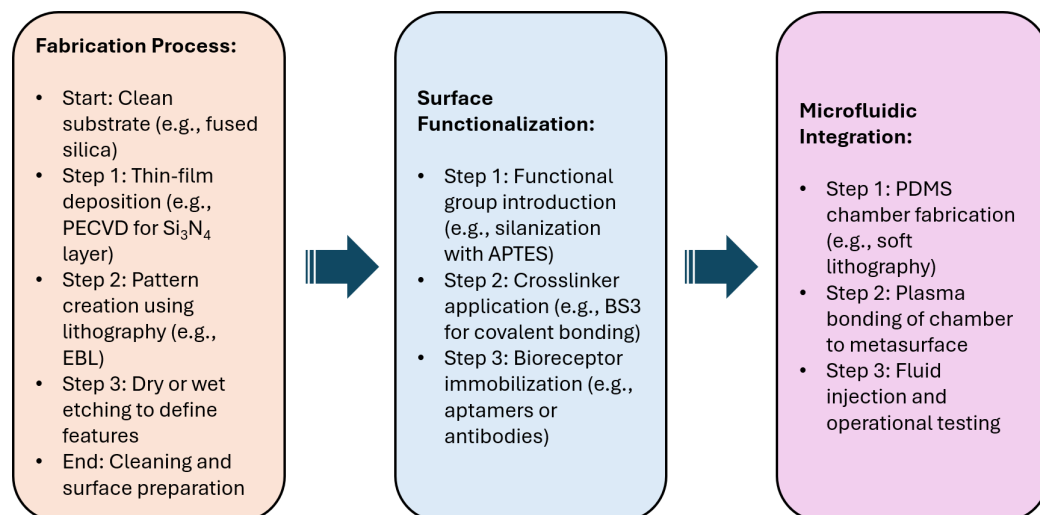


Figure 4. Overview of the fabrication, functionalization, and integration processes for BIC-based metasurfaces for biosensing.

5. Applications of BIC-Based Biosensors

As widely discussed in this paper, BIC-based biosensors leverage the unique properties of high-Q resonances and enhanced light–matter interactions to achieve exceptional performance metrics. These sensors have demonstrated transformative potential across various application domains, including clinical diagnostics, environmental monitoring, and food safety. This section provides an in-depth discussion of the performance parameters critical for biosensor applications, followed by an analysis of experimental results from BIC-based biosensors.

5.1. Key Performance Metrics for Biosensors

The performance of a biosensor is determined by several critical parameters, which define its suitability for specific applications. Among these, the LoD and dynamic range are the most fundamental metrics, but sensitivity, specificity, and time of response also play vital roles.

The LoD represents the smallest concentration of analyte that a biosensor can reliably detect. For BIC-based sensors, LoD is significantly enhanced by their high-Q resonances, which amplify the interaction between the analyte and the functionalized surface.

Dynamic range refers to the range of analyte concentrations over which the sensor provides accurate and linear detection. A wide dynamic range is essential for biosensors used in clinical and environmental monitoring, where analyte concentrations can vary significantly. BIC-based biosensors typically exhibit dynamic ranges spanning several orders of magnitude, ensuring their applicability across diverse scenarios.

Sensitivity quantifies the sensor's ability to detect small changes in analyte concentration. In BIC-based biosensors, sensitivity is often expressed as the shift in resonance wavelength per unit change in refractive index (nm/RIU).

Specificity refers to the ability of the biosensor to distinguish the target analyte from other substances in complex samples. BIC-based sensors achieve high specificity through advanced functionalization strategies, such as the use of molecularly imprinted polymers, aptamers, or antibodies, which selectively bind to the target analyte. The strong field confinement provided by BICs further enhances specificity by increasing binding affinity.

The time required for a biosensor to detect and quantify an analyte is critical in applications requiring real-time monitoring. BIC-based sensors generally offer rapid response times due to their highly localized field interactions, enabling quick and efficient analyte detection. Reported response times range from a few seconds to minutes, depending on the target analyte and functionalization method.

5.2. Experimental Applications of BIC-Based Biosensors

The unique properties of BIC-based biosensors have enabled their use in a variety of real-world applications. Experimental evidence highlights their effectiveness in clinical diagnostics, environmental monitoring, and food safety. Table 1 summarizes the experimental performance metrics of some highly representative recent BIC-based biosensors, highlighting their LoD, sensitivity, and Q-factors across various applications. Figure 5 provides a graphical summary of their application domains and performance metrics. The results presented in Table 1 highlight and confirm the trade-offs and advantages of different approaches for BIC-based biosensors. For instance, dielectric metasurfaces exhibit higher Q-factors due to their low intrinsic optical losses. On the other hand, hybrid systems combine the strengths of plasmonic and dielectric structures. These systems achieve significant near-field enhancement due to plasmonic effects while maintaining relatively low losses. Although their Q-factors are slightly lower than purely dielectric structures, hybrid metasurfaces offer advantages in detecting biomolecules at extremely low concentrations, as evidenced by LoDs in the zeptomolar range.

BIC-based biosensors have shown exceptional potential in detecting biomarkers at ultra-low concentrations, facilitating early diagnosis of diseases. For instance, Clabassi et al. [57] utilized a hybrid BIC sensor to detect transactive response DNA-binding protein 43 (TDP-43), a biomarker for neurodegenerative diseases, especially amyotrophic lateral sclerosis, achieving an LoD of 100 zM and a detection range ranging from 100 fM to 100 zM.

Zito et al. [58] demonstrated the detection of the transforming growth factor-beta (TGF-beta) at 10 fM in saliva, showcasing the applicability of BIC sensors in non-invasive diagnostics. The result is particularly interesting due to the use of MIP as a biorecognition element and the clinical relevance of the target biomarker, a cytokine, which is involved in the progression of oral cancer.

In environmental and food safety applications, BIC-based sensors have been employed to detect pathogens, toxins, allergens, pollutants, and contaminants with high precision. Schiattarella et al. [59] reported the detection of ochratoxin A in food products with an LoD of 2.3 pg/mL (=5.7 pM), highlighting their capability for ensuring compliance with safety standards. Ochratoxin A has nephrotoxic, immunotoxic, carcinogenic, and genotoxic effects. Thus, its detection, also at the level of traces, is crucial in many application contexts. Sensors based on the same operating principle or similar ones are also being explored for real-time monitoring of heavy metals and pesticides in water and air samples.

Table 1. Comparative performance of BIC-based biosensors in experimental studies.

Study	Target Analyte	LoD
Zito et al., 2024 [58]	TGF-beta	10 fM
Clabassi et al., 2024 [57]	TDP-43	100 zM
Schiattarella et al., 2022 [59]	Ochratoxin A	6 pM

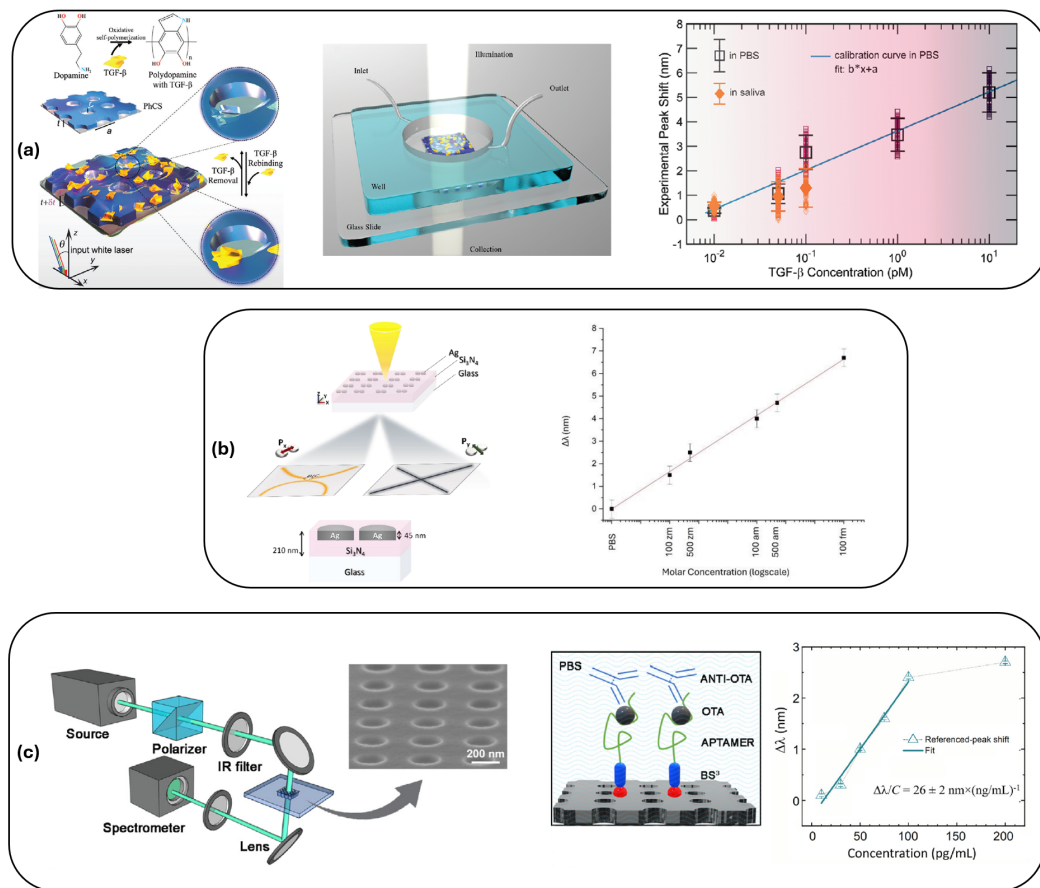


Figure 5. Graphical summary of experimental achievements and application areas for BIC-based biosensors, including clinical diagnostics, environmental monitoring, and food safety. (a) Scheme of an MIP–BIC biosensor for TGF-beta detection, showing the interrogation scheme and dose-response curve (LoD = 10 fM [58]). (b) Nanostructure based on dimers for hybrid symmetry-protected BIC generation, consisting of a square array of fully silver-filled nanoholes within a silicon nitride waveguide slab. The dose-response curve is provided (LoD = 100 zM [57]). (c) Sensing setup with an SEM image of the metasurface and a schematic of surface functionalization. A spectral shift vs. ochratoxin A concentration is shown (LoD = 6 pM [59]). Reprinted with permission from [57–59].

6. Future Directions, Challenges, and Conclusions

BIC-based biosensors hold immense promise for applications requiring high sensitivity, low detection limits, and precise specificity, particularly in fields such as clinical diagnostics, environmental monitoring, and food safety. Despite these advantages, the broader application and commercialization of BIC-based biosensors require addressing several technological challenges and leveraging emerging trends to enhance their functionality and adaptability. Key areas for future research include the development of hybrid BIC sensors, improving scalability, integrating with microfluidics, and advancing functionalization and multiplexing capabilities. Also, integration with hyperspectral imaging has already proven its promise with the experimental demonstration of biomolecular detection information at the extremely low molecular counts of approximately three molecules per μm^2 [22].

One of the most promising advancements in BIC-based biosensors is the integration of hybrid structures that combine BIC resonances with advanced materials, such as MIPs. MIPs offer selective binding sites that serve as a “molecular fingerprint” for target analytes, thereby enhancing the sensor’s specificity. By incorporating MIPs into BIC structures, sensors can achieve greater selectivity and stability, making them especially suited for applications where high specificity is required. Additionally, materials like graphene and transition metal dichalcogenides offer unique properties that can be harnessed to further

customize BIC sensors. Graphene's tunable electrical and optical properties, for instance, can facilitate dynamic control of BIC resonances, enabling real-time adjustments in sensing applications and further broadening the capabilities of BIC-based sensors.

Scalability remains a significant challenge in the development of BIC-based biosensors, especially for large-scale production. While high-precision fabrication techniques such as electron beam lithography and focused ion beam milling are effective for research purposes, their low throughput and high costs limit their feasibility for mass production. Nanoimprint lithography has emerged as a promising alternative, offering the ability to replicate high-resolution features over large areas with reduced costs. However, achieving consistent high-Q performance across large surfaces using NIL remains challenging, as even minor variations in mold quality or pressure can impact the uniformity of the BIC structures. Addressing these issues is crucial for enabling large-scale production of BIC sensors that maintain high sensitivity and reliable performance, paving the way for widespread use in commercial and industrial applications.

The integration of BIC-based biosensors with microfluidic systems presents another frontier for innovation, particularly for point-of-care testing in medical and environmental applications. Microfluidic platforms allow precise control over small fluid volumes, enabling efficient sample handling and on-site testing. By combining BIC sensors with microfluidics, it is possible to develop portable diagnostic devices capable of rapid, real-time analysis in decentralized settings, thus reducing the dependency on centralized laboratories. However, integrating BIC structures with microfluidic channels involves significant technical challenges, including alignment, material compatibility, and maintaining sensor stability over extended use. Successfully addressing these integration challenges could expand the accessibility and utility of BIC-based sensors in healthcare, offering faster diagnostics and improved patient outcomes.

Further advancements in functionalization methods could also enhance the specificity and applicability of BIC biosensors. Current functionalization techniques, such as using antibodies, aptamers, or molecularly imprinted polymers, provide a degree of selectivity that is crucial for accurate detection. However, new strategies involving multi-layered functionalization or combinatorial libraries could push the boundaries of selectivity even further, enabling BIC sensors to accurately distinguish between structurally similar biomolecules. This would be particularly beneficial for clinical diagnostics, where high specificity is required to detect disease markers in complex biological samples. Additionally, advances in multiplexing could enable BIC-based sensors to detect multiple analytes simultaneously, which is invaluable in medical diagnostics where profiling multiple biomarkers can provide a comprehensive health assessment.

The miniaturization of BIC-based sensor systems is another area with transformative potential. By integrating compact light sources, detectors, and readout electronics with BIC structures, it is feasible to create portable devices for field diagnostics and point-of-care applications. Such miniaturized systems could allow BIC biosensors to be deployed in resource-limited or remote settings, providing rapid and accurate testing capabilities where laboratory facilities are unavailable. The portability and ease of use of such devices would not only broaden the applicability of BIC sensors but also help to address healthcare disparities by improving access to diagnostics in underserved regions.

In conclusion, BIC-based biosensors have demonstrated clear advantages over traditional sensing technologies, offering higher sensitivity, lower detection limits, and superior specificity through enhanced light confinement and selective functionalization. These attributes position BIC-based sensors as a transformative tool in biosensing, with potential applications across diagnostics, environmental monitoring, and food safety. Nonetheless, challenges in scalability, material integration, and device miniaturization remain. Ad-

addressing these challenges will require a collaborative effort across disciplines, combining advancements in nanofabrication, materials science, and microfluidics to fully realize the potential of BIC technology.

Looking forward, BIC-based biosensors are poised to play a significant role in next-generation biosensing and diagnostic applications. The ongoing exploration of hybrid materials, improved fabrication techniques, and integration strategies will likely expand the scope and functionality of BIC sensors, making them increasingly competitive in the biosensor industry. As these advancements continue, BIC technology is expected to drive innovation in diagnostics and environmental sensing, offering more sensitive, specific, and accessible biosensing solutions that meet the growing demands of modern healthcare and environmental safety.

As already mentioned, the two key performance parameters of a biosensor are the LoD and the dynamic range. Significant improvements in these metrics can be achieved by enhancing the Q-factor through innovative metasurface designs and, more critically, through the optimization of fabrication techniques to reduce imperfections that limit the Q-factor.

Additionally, improving the quality and specificity of biological receptors—as well as functionalization strategies—can enhance the sensitivity and ensure reliable detection of low-concentration analytes. Advanced functionalization methods, including multi-layered biointerfaces, could further amplify performance by increasing selectivity.

Another key direction is extending the dynamic range of the sensor, ensuring operation across a broader range of analyte concentrations. This could be achieved by introducing hybrid sensor designs that combine BIC resonances with mechanisms for controlled field localization, thereby maintaining high sensitivity even at elevated analyte levels.

The stability and reusability of BIC-based biosensors are key factors for their practical deployment, particularly in applications such as point-of-care diagnostics. While extensive stability tests are beyond the scope of this review, several referenced studies suggest promising durability and operational robustness. For instance, Schiattarella et al. demonstrated consistent performance over multiple sensing cycles [59], while Romano et al. highlighted the mechanical stability of microfluidic systems integrated with BIC metasurfaces [45]. These findings indicate the potential for the reliable long-term use of BIC-based biosensors under typical operational conditions.

Funding: F.D. acknowledges the support of the project PRIN-2022 ALPHA “ALI-dielectric resonant metasurfaces enhancing PHoton emission phenomena” (CUP:D53D23001060006) funded by the Italian Ministry of University and Research. F.D. acknowledges the support of the European Union under the Italian National Recovery and Resilience Plan (NRRP) of Next Generation EU, partnership on “Telecommunications of the Future” (PE00000001—program “RESTART”).

Conflicts of Interest: The author declares no conflicts of interest.

References

1. Pasquarelli, A. *Biosensors and Biochips*, 1st ed.; Learning Materials in Biosciences; Springer International Publishing: Berlin/Heidelberg, Germany, 2021. [CrossRef]
2. Preston, K.J.; Chen, G.; Chapman, C.A.; Gundavarapu, S.; Aljohani, E.; Paredes Arroyo, A.; Lin, C.C.; Vinitzky, A.; Gonzales, A.; Yin, Z.; et al. At-home measurement of blood biomarkers on the SiPhox Home silicon photonics platform. In *Proceedings of the Frontiers in Biological Detection: From Nanosensors to Systems XVI*; Miller, B.L., Weiss, S.M., Danielli, A., Eds.; SPIE: Bellingham, WA, USA, 2024; p. 6. [CrossRef]
3. Steiner, D.J.; Bryan, M.R.; Miller, B.L. Photonic biosensing at the point-of-care. In *Biophotonics and Biosensing*; Elsevier: Amsterdam, The Netherlands, 2024; pp. 243–268. [CrossRef]
4. Yu, N.; Capasso, F. Flat optics with designer metasurfaces. *Nat. Mater.* **2014**, *13*, 139–150. [CrossRef] [PubMed]

5. Kildishev, A.V.; Boltasseva, A.; Shalae, V.M. Planar Photonics with Metasurfaces. *Science* **2013**, *339*, 1232009. [[CrossRef](#)] [[PubMed](#)]
6. Khorasaninejad, M.; Capasso, F. Metalenses at visible wavelengths: Diffraction-limited focusing and subwavelength resolution imaging. *Science* **2016**, *352*, 1190–1194. [[CrossRef](#)]
7. Genevet, P.; Capasso, F.; Aieta, F.; Khorasaninejad, M.; Devlin, R. Recent advances in planar optics: From plasmonic to dielectric metasurfaces. *Optica* **2017**, *4*, 139. [[CrossRef](#)]
8. Schulz, S.A.; Oulton, R.F.; Kenney, M.; Alù, A.; Staude, I.; Bashiri, A.; Fedorova, Z.; Kolkowski, R.; Koenderink, A.F.; Xiao, X.; et al. Roadmap on photonic metasurfaces. *Appl. Phys. Lett.* **2024**, *124*, 260701. [[CrossRef](#)]
9. Kuznetsov, A.I.; Brongersma, M.L.; Yao, J.; Chen, M.K.; Levy, U.; Tsai, D.P.; Zheludev, N.I.; Faraon, A.; Arbabi, A.; Yu, N.; et al. Roadmap for Optical Metasurfaces. *ACS Photonics* **2024**, *11*, 816–865. [[CrossRef](#)]
10. Yuan, L.; Zhao, Y.; Toma, A.; Aglieri, V.; Gerislioglu, B.; Yuan, Y.; Lou, M.; Ogundare, A.; Alabastri, A.; Nordlander, P.; et al. A Quasi-Bound States in the Continuum Dielectric Metasurface-Based Antenna–Reactor Photocatalyst. *Nano Lett.* **2023**, *24*, 172–179. [[CrossRef](#)]
11. Yu, S.; Xu, M.; Pu, M.; Tang, X.; Zheng, Y.; Guo, Y.; Zhang, F.; Li, X.; Ma, X.; Luo, X. Dynamic nonlocal metasurface for multifunctional integration via phase-change materials. *Nanophotonics* **2024**, *13*, 4317–4325. [[CrossRef](#)] [[PubMed](#)]
12. Chen, Y.; Liu, Z.; Li, Y.; Hu, Z.; Wu, J.; Wang, J. Adjustable converter of bound state in the continuum basing on metal-graphene hybrid metasurfaces. *Opt. Express* **2022**, *30*, 23828. [[CrossRef](#)] [[PubMed](#)]
13. Zhang, S.; Wong, C.L.; Zeng, S.; Bi, R.; Tai, K.; Dholakia, K.; Olivo, M. Metasurfaces for biomedical applications: Imaging and sensing from a nanophotonics perspective. *Nanophotonics* **2020**, *10*, 259–293. [[CrossRef](#)]
14. Tseng, M.L.; Jahani, Y.; Leitis, A.; Altug, H. Dielectric Metasurfaces Enabling Advanced Optical Biosensors. *ACS Photonics* **2020**, *8*, 47–60. [[CrossRef](#)]
15. Chung, T.; Wang, H.; Cai, H. Dielectric metasurfaces for next-generation optical biosensing: A comparison with plasmonic sensing. *Nanotechnology* **2023**, *34*, 402001. [[CrossRef](#)] [[PubMed](#)]
16. Altug, H.; Oh, S.H.; Maier, S.A.; Homola, J. Advances and applications of nanophotonic biosensors. *Nat. Nanotechnol.* **2022**, *17*, 5–16. [[CrossRef](#)] [[PubMed](#)]
17. Hsu, C.W.; Zhen, B.; Stone, A.D.; Joannopoulos, J.D.; Soljačić, M. Bound states in the continuum. *Nat. Rev. Mater.* **2016**, *1*, 16048. [[CrossRef](#)]
18. Liu, Z.; Wang, K.; Zhang, Y.; Mao, D. High-Q quasi-bound states in the continuum for nonlinear metasurfaces. *Phys. Rev. Lett.* **2019**, *123*, 253901. [[CrossRef](#)]
19. Koshelev, K.; Bogdanov, A.; Kivshar, Y. Meta-optics and bound states in the continuum. *Sci. Bull.* **2019**, *64*, 836–842. [[CrossRef](#)] [[PubMed](#)]
20. Tan, Z.; Su, M.; Song, Y. Metamaterials-tuned light-matter resonance for ultra-sensitivity biological diagnosis. *Matter* **2024**, *7*, 2657–2659. [[CrossRef](#)]
21. Khan, S.A.; Khan, N.Z.; Xie, Y.; Abbas, M.T.; Rauf, M.; Mehmood, I.; Runowski, M.; Agathopoulos, S.; Zhu, J. Optical Sensing by Metamaterials and Metasurfaces: From Physics to Biomolecule Detection. *Adv. Opt. Mater.* **2022**, *10*, 2200500. [[CrossRef](#)]
22. Yesilkoy, F.; Arvelo, E.R.; Jahani, Y.; Liu, M.; Tittl, A.; Cevher, V.; Kivshar, Y.; Altug, H. Ultrasensitive hyperspectral imaging and biodetection enabled by dielectric metasurfaces. *Nat. Photonics* **2019**, *13*, 390–396. [[CrossRef](#)]
23. Algorri, J.F.; Dell’Olio, F.; Roldán-Varona, P.; Rodríguez-Cobo, L.; López-Higuera, J.M.; Sánchez-Pena, J.M.; Zografopoulos, D.C. Strongly resonant silicon slot metasurfaces with symmetry-protected bound states in the continuum. *Opt. Express* **2021**, *29*, 10374. [[CrossRef](#)]
24. Algorri, J.F.; Dell’Olio, F.; Roldán-Varona, P.; Rodríguez-Cobo, L.; López-Higuera, J.M.; Sánchez-Pena, J.M.; Dmitriev, V.; Zografopoulos, D.C. Analogue of electromagnetically induced transparency in square slotted silicon metasurfaces supporting bound states in the continuum. *Opt. Express* **2022**, *30*, 4615. [[CrossRef](#)]
25. Algorri, J.; Dmitriev, V.; Hernández-Figueroa, H.; Rodríguez-Cobo, L.; Dell’Olio, F.; Cusano, A.; López-Higuera, J.; Zografopoulos, D. Polarization-independent hollow nanocuboid metasurfaces with robust quasi-bound states in the continuum. *Opt. Mater.* **2024**, *147*, 114631. [[CrossRef](#)]
26. Zhou, Y.; Guo, Z.; Zhao, X.; Wang, F.; Yu, Z.; Chen, Y.; Liu, Z.; Zhang, S.; Sun, S.; Wu, X. Dual-Quasi Bound States in the Continuum Enabled Plasmonic Metasurfaces. *Adv. Opt. Mater.* **2022**, *10*, 2200965. [[CrossRef](#)]
27. Lyu, J.; Huang, L.; Chen, L.; Zhu, Y.; Zhuang, S. Review on the terahertz metasensor: From featureless refractive index sensing to molecular identification. *Photonics Res.* **2024**, *12*, 194. [[CrossRef](#)]
28. Wang, R.; Xu, L.; Huang, L.; Zhang, X.; Ruan, H.; Yang, X.; Lou, J.; Chang, C.; Du, X. Ultrasensitive Terahertz Biodetection Enabled by Quasi-BIC-Based Metasensors. *Small* **2023**, *19*, 2301165. [[CrossRef](#)] [[PubMed](#)]
29. Zhang, W.; Lin, J.; Yuan, Z.; Lin, Y.; Shang, W.; Chin, L.K.; Zhang, M. Terahertz Metamaterials for Biosensing Applications: A Review. *Biosensors* **2023**, *14*, 3. [[CrossRef](#)] [[PubMed](#)]
30. Stillinger, F.H.; Herrick, D.R. Bound states in the continuum. *Phys. Rev. A* **1975**, *11*, 446–454. [[CrossRef](#)]

31. Marinica, D.C.; Borisov, A.G.; Shabanov, S.V. Bound States in the Continuum in Photonics. *Phys. Rev. Lett.* **2008**, *100*, 183902. [[CrossRef](#)] [[PubMed](#)]
32. Kang, M.; Liu, T.; Chan, C.T.; Xiao, M. Applications of bound states in the continuum in photonics. *Nat. Rev. Phys.* **2023**, *5*, 659–678. [[CrossRef](#)]
33. Plotnik, Y.; Peleg, O.; Dreisow, F.; Heinrich, M.; Nolte, S.; Szameit, A.; Segev, M. Experimental Observation of Optical Bound States in the Continuum. *Phys. Rev. Lett.* **2011**, *107*, 183901. [[CrossRef](#)] [[PubMed](#)]
34. Li, S.; Zhou, C.; Liu, T.; Xiao, S. Symmetry-protected bound states in the continuum supported by all-dielectric metasurfaces. *Phys. Rev. A* **2019**, *100*, 063803. [[CrossRef](#)]
35. Huang, L.; Li, S.; Zhou, C.; Zhong, H.; You, S.; Li, L.; Cheng, Y.; Miroshnichenko, A.E. Realizing Ultrahigh-Q Resonances Through Harnessing Symmetry-Protected Bound States in the Continuum. *Adv. Funct. Mater.* **2024**, *34*, 2309982. [[CrossRef](#)]
36. Sadrieva, Z.F.; Belyakov, M.A.; Balezin, M.A.; Kapitanova, P.V.; Nenasheva, E.A.; Sadreev, A.F.; Bogdanov, A.A. Experimental observation of a symmetry-protected bound state in the continuum in a chain of dielectric disks. *Phys. Rev. A* **2019**, *99*, 053804. [[CrossRef](#)]
37. Neale, S.; Muljarov, E.A. Accidental and symmetry-protected bound states in the continuum in a photonic-crystal slab: A resonant-state expansion study. *Phys. Rev. B* **2021**, *103*, 155112. [[CrossRef](#)]
38. Sidorenko, M.; Sergaeva, O.; Sadrieva, Z.; Roques-Carmes, C.; Muraev, P.; Maksimov, D.; Bogdanov, A. Observation of an Accidental Bound State in the Continuum in a Chain of Dielectric Disks. *Phys. Rev. Appl.* **2021**, *15*, 034041. [[CrossRef](#)]
39. Amrani, M.; Khattou, S.; El Boudouti, E.H.; Talbi, A.; Akjouj, A.; Dobrzynski, L.; Djafari-Rouhani, B. Friedrich-Wintgen bound states in the continuum and induced resonances in a loop laterally coupled to a waveguide. *Phys. Rev. B* **2022**, *106*, 125414. [[CrossRef](#)]
40. Luo, M.; Wu, F. Wavy optical grating: Wideband reflector and Fabry-Pérot bound states in the continuum. *Phys. Rev. A* **2022**, *106*, 063514. [[CrossRef](#)]
41. Nabol, S.V.; Pankin, P.S.; Maksimov, D.N.; Timofeev, I.V. Fabry-Perot bound states in the continuum in an anisotropic photonic crystal. *Phys. Rev. B* **2022**, *106*, 245403. [[CrossRef](#)]
42. Li, X.; Maqbool, E.; Han, Z. Narrowband mid-infrared thermal emitters based on the Fabry-Perot type of bound states in the continuum. *Optics Express* **2023**, *31*, 20338. [[CrossRef](#)] [[PubMed](#)]
43. Jin, J.; Yin, X.; Ni, L.; Soljačić, M.; Zhen, B.; Peng, C. Topologically enabled ultrahigh-Q guided resonances robust to out-of-plane scattering. *Nature* **2019**, *574*, 501–504. [[CrossRef](#)] [[PubMed](#)]
44. Algorri, J.F.; Dell’Olio, F.; Ding, Y.; Labbé, F.; Dmitriev, V. Experimental demonstration of a silicon-slot quasi-bound state in the continuum in near-infrared all-dielectric metasurfaces. *Opt. Laser Technol.* **2023**, *161*, 109199. [[CrossRef](#)]
45. Romano, S.; Zito, G.; Torino, S.; Calafiore, G.; Penzo, E.; Coppola, G.; Cabrini, S.; Rendina, I.; Mocella, V. Label-free sensing of ultralow-weight molecules with all-dielectric metasurfaces supporting bound states in the continuum. *Photonics Res.* **2018**, *6*, 726. [[CrossRef](#)]
46. Conteduca, D.; Arruda, G.S.; Barth, I.; Wang, Y.; Krauss, T.F.; Martins, E.R. Beyond Q: The Importance of the Resonance Amplitude for Photonic Sensors. *ACS Photonics* **2022**, *9*, 1757–1763. [[CrossRef](#)]
47. Luo, M.; Zhou, Y.; Zhao, X.; Guo, Z.; Li, Y.; Wang, Q.; Liu, J.; Luo, W.; Shi, Y.; Liu, A.Q.; et al. High-Sensitivity Optical Sensors Empowered by Quasi-Bound States in the Continuum in a Hybrid Metal–Dielectric Metasurface. *ACS Nano* **2024**, *18*, 6477–6486. [[CrossRef](#)] [[PubMed](#)]
48. Lalanne, P.; Morris, G.M. Highly improved convergence of the coupled-wave method for TM polarization. *JOSA A* **1996**, *13*, 779. [[CrossRef](#)]
49. Lalanne, P. Convergence performance of the coupled-wave and the differential methods for thin gratings. *JOSA A* **1997**, *14*, 1583. [[CrossRef](#)]
50. Lalanne, P. Improved formulation of the coupled-wave method for two-dimensional gratings. *JOSA A* **1997**, *14*, 1592. [[CrossRef](#)]
51. Lalanne, P.; Jurek, M.P. Computation of the near-field pattern with the coupled-wave method for transverse magnetic polarization. *J. Mod. Opt.* **1998**, *45*, 1357–1374. [[CrossRef](#)]
52. Silberstein, E.; Lalanne, P.; Hugonin, J.P.; Cao, Q. Use of grating theories in integrated optics. *JOSA A* **2001**, *18*, 2865. [[CrossRef](#)]
53. Yao, Y.; Liu, H.; Wang, Y.; Li, Y.; Song, B.; Wang, R.P.; Povinelli, M.L.; Wu, W. Nanoimprint-defined, large-area meta-surfaces for unidirectional optical transmission with superior extinction in the visible-to-infrared range. *Opt. Express* **2016**, *24*, 15362. [[CrossRef](#)] [[PubMed](#)]
54. Choi, S.; Zuo, J.; Das, N.; Yao, Y.; Wang, C. Scalable Nanoimprint Manufacturing of Functional Multilayer Metasurface Devices. *Adv. Funct. Mater.* **2024**, *34*, 2404852. [[CrossRef](#)]
55. Oh, D.K.; Lee, T.; Ko, B.; Badloe, T.; Ok, J.G.; Rho, J. Nanoimprint lithography for high-throughput fabrication of metasurfaces. *Front. Optoelectron.* **2021**, *14*, 229–251. [[CrossRef](#)]

56. Einck, V.J.; Torfeh, M.; McClung, A.; Jung, D.E.; Mansouree, M.; Arbabi, A.; Watkins, J.J. Scalable Nanoimprint Lithography Process for Manufacturing Visible Metasurfaces Composed of High Aspect Ratio TiO₂ Meta-Atoms. *ACS Photonics* **2021**, *8*, 2400–2409. [[CrossRef](#)]
57. Clabassi, E.; Balestra, G.; Siciliano, G.; Polimeno, L.; Tarantini, I.; Primiceri, E.; Tobaldi, D.M.; Cuscunà, M.; Quaranta, F.; Passaseo, A.; et al. Hybrid plasmonic Bound State in the Continuum entering the zeptomolar biodetection range. *arXiv* **2024**. [[CrossRef](#)]
58. Zito, G.; Siciliano, G.; Seifalinezhad, A.; Miranda, B.; Lanzio, V.; Schwartzberg, A.; Gigli, G.; Turco, A.; Rendina, I.; Mocella, V.; et al. Molecularly Imprinted Polymer Sensor Empowered by Bound States in the Continuum for Selective Trace-Detection of TGF-beta. *Adv. Sci.* **2024**, *11*, 2401843. [[CrossRef](#)] [[PubMed](#)]
59. Schiattarella, C.; Sanità, G.; Guilcapi Alulema, B.; Lanzio, V.; Cabrini, S.; Lamberti, A.; Rendina, I.; Mocella, V.; Zito, G.; Romano, S. High-Q photonic aptasensor based on avoided crossing bound states in the continuum and trace detection of ochratoxin A. *Biosens. Bioelectron. X* **2022**, *12*, 100262. [[CrossRef](#)]

Disclaimer/Publisher's Note: The statements, opinions and data contained in all publications are solely those of the individual author(s) and contributor(s) and not of MDPI and/or the editor(s). MDPI and/or the editor(s) disclaim responsibility for any injury to people or property resulting from any ideas, methods, instructions or products referred to in the content.